Deep Learning in Radiology: Applications in Lesion and Organ Segmentation

Yuxing Tang, Youbao Tang

14 February 2019

Imaging Biomarkers and Computer-Aided Diagnosis Laboratory,
Department of Radiology and Imaging Sciences,
National Institutes of Health Clinical Center, Bethesda, MD 20892, USA

CAD Lab @ NIH Clinical Center

Ronald M. Summers, M.D., Ph.D.

Senior Investigator

Imaging Biomarkers and Computer-Aided Diagnosis Laboratory

NIH Clinical Center

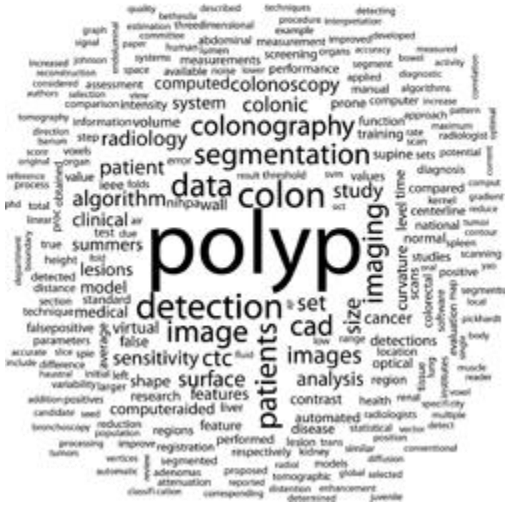

Overview

- Background
- Previous work in our lab
- Lesion & organ segmentation
- Fully supervised vs. weakly supervised learning
- Generative adversarial networks (GANs) for data augmentation and segmentation

Computer-Aided Diagnosis

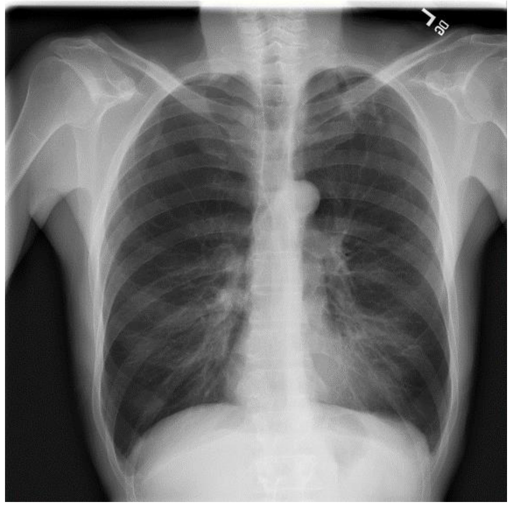
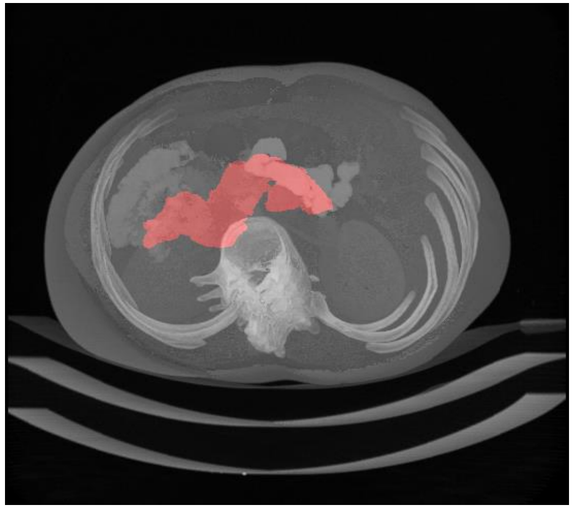
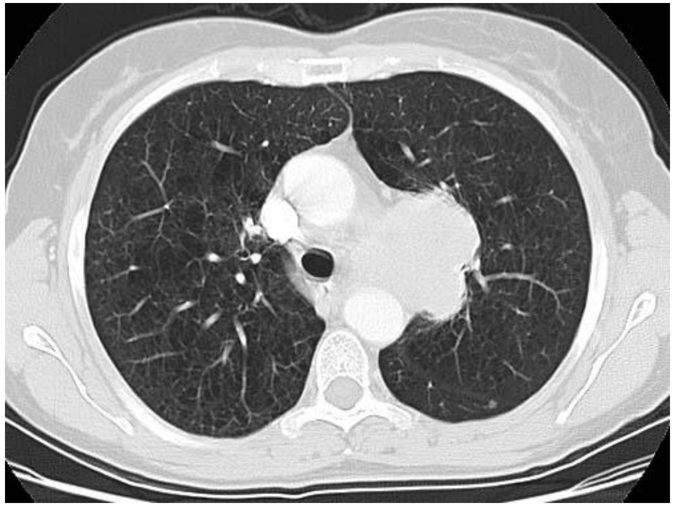
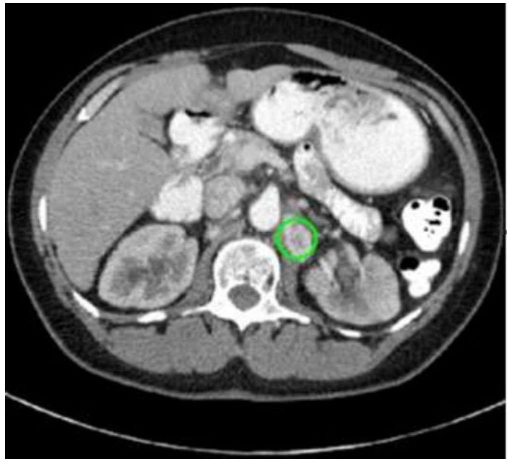
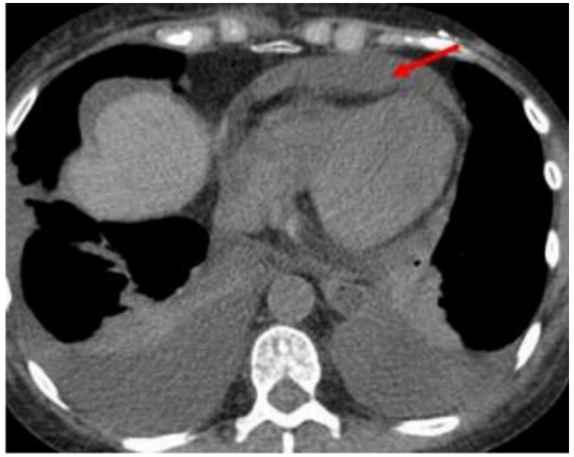
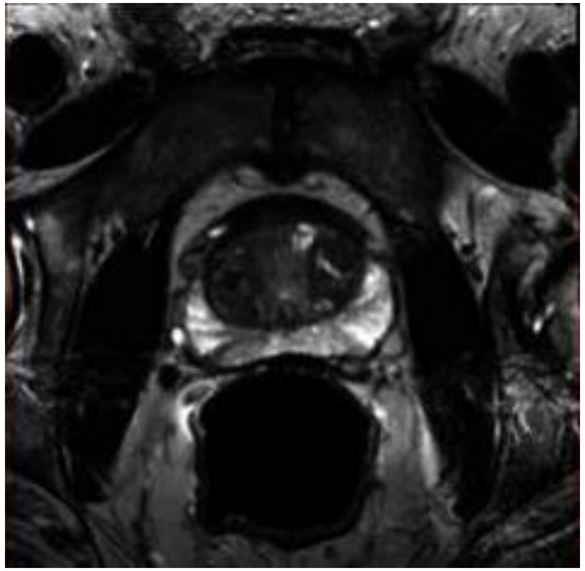

Era of Deep Learning

- No more hand-crafted features
- Large-scale annotated datasets
- Impact: More and varied researchers can contribute, accelerating pace of progress

Deep Learning Improves CAD

Journals & Magazines > IEEE Transactions on Medical ... > Volume: 35 Issue: 5

Guest Editorial Deep Learning in Medical Imaging: Overview and Future Promise of an Exciting New Technique

3 Author(s) Hayit Greenspan ; Bram van Ginneken ; Ronald M. Summers

Computer-Aided Diagnosis with Deep Learning Architecture: Applications to Breast Lesions in US Images and Pulmonary Nodules in CT Scans

Jie-Zhi Cheng, Dong Ni, Yi-Hong Chou, Jing Qin, Chui-Mei Tiu, Yeun-Chung Chang, Chiun-Sheng Huang, Dinggang Shen & Chung-Ming Chen

Scientific Reports **6**, Article number: 24454 (2016) | Download Citation

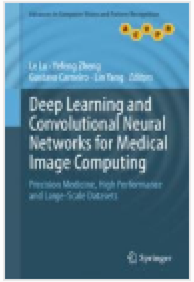

Deep Learning and Convolutional Neural Networks for Medical Image Com

Deep Learning and Computer-Aided Diagnosis for Medical Image Processing: A Personal Perspective

Authors | Authors and affiliations

Ronald M. Summers 1
Email author

1. Imaging Biomarkers and Computer-Aided Diagnosis Laboratory, Radiology and Imaging Sciences, National Institutes of Health Clinical Center, Bethesda, USA

CT Pancreas Segmentation

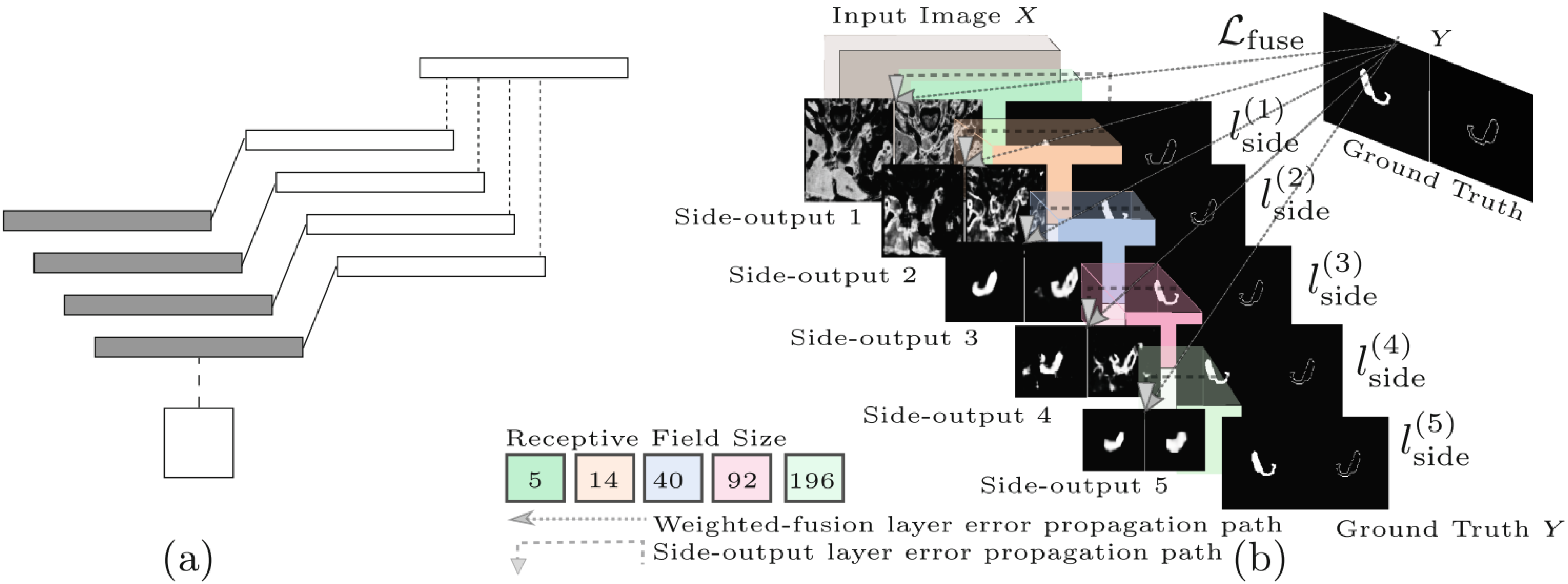

H. Roth et al. *Spatial Aggregation of Holistically-Nested Networks for Automated Pancreas Segmentation*, MICCAI 2016

CT Pancreas Segmentation

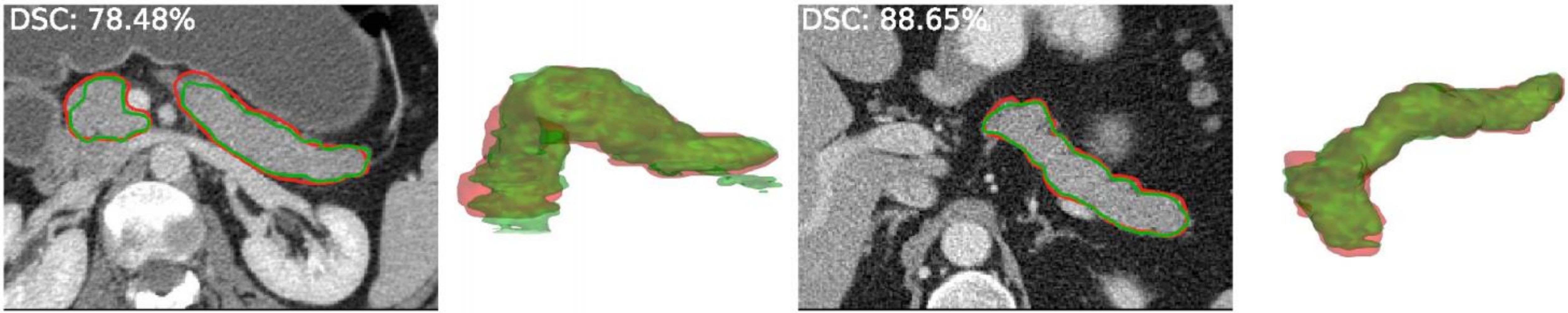

H. Roth et al. *Spatial Aggregation of Holistically-Nested Networks for Automated Pancreas Segmentation*, MICCAI 2016

Pancreas CT Dataset

- Abdominal contrast enhanced CT scans
- 82 patients
- Manual annotations
- DICOM, 10 GB


THE CANCER IMAGING ARCHIVE

HOME NEWS ABOUT US SUBMIT YOUR DATA ACCESS THE DATA RESEARCH ACTIVITIES

Confluence Spaces Search

The Cancer Imaging Archive (TCIA) Public Access

Blog

SPACE SHORTCUTS

How-to articles

Troubleshooting articles

CHILD PAGES

Collections

Pancreas-CT

Dashboard / Wiki / Collections

Pancreas-CT

Created by smberryman, last modified by Klingerc on Nov 20, 2018

Summary

The National Institutes of Health Clinical Center performed 82 abdominal contrast enhanced 3D CT scans (~70 seconds after intravenous contrast injection in portal-venous) from 53 male and 27 female subjects. Seventeen of the subjects are healthy kidney donors scanned prior to nephrectomy. The remaining 65 patients were selected by a radiologist from patients who neither had major abdominal pathologies nor pancreatic cancer lesions. Subjects' ages range from 18 to 76 years with a mean age of 46.8 ± 16.7. The CT scans have resolutions of 512x512 pixels with varying pixel sizes and slice thickness between 1.5 − 2.5 mm, acquired on Philips and Siemens MDCT scanners (120 kVp tube voltage).

A medical student manually performed slice-by-slice segmentations of the pancreas as ground-truth and these were verified/modified by an experienced radiologist.

https://wiki.cancerimagingarchive.net/display/Public/Pancreas-CT

CT Lymph Node Segmentation

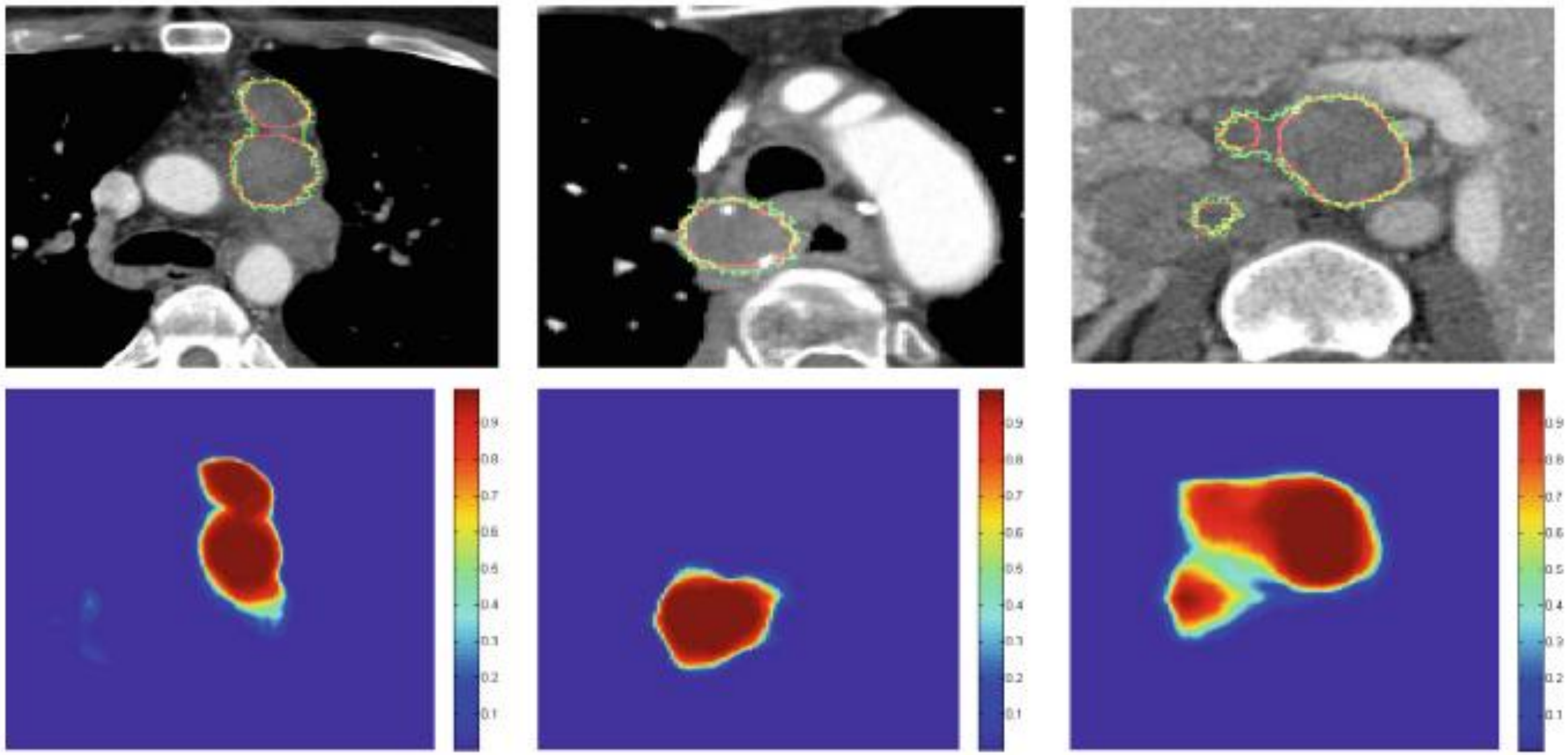

I. Nogues et al. *Automatic Lymph Node Cluster Segmentation Using Holistically-Nested Neural Networks and Structured Optimization in CT Images*, MICCAI 2016

Lymph Node CT Dataset

- Computed Tomography (CT) images of the mediastinum and abdomen
- 176 patient scans
- ~1,000 lymph node masks annotated by radiologist
- DICOM, 58 GB

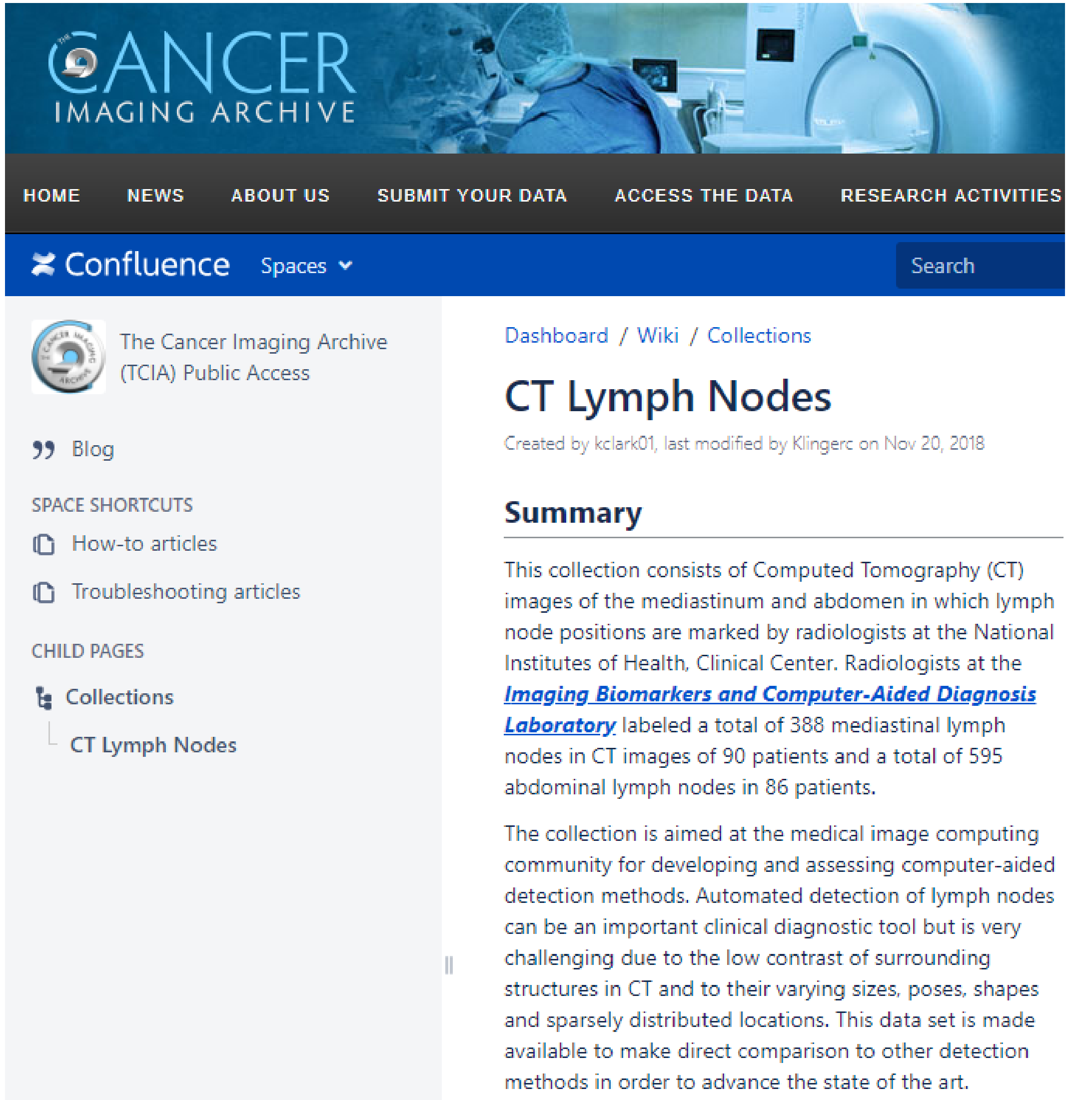

https://wiki.cancerimagingarchive.net/display/Public/CT+Lymph+Nodes

Chest CT Lung Segmentation

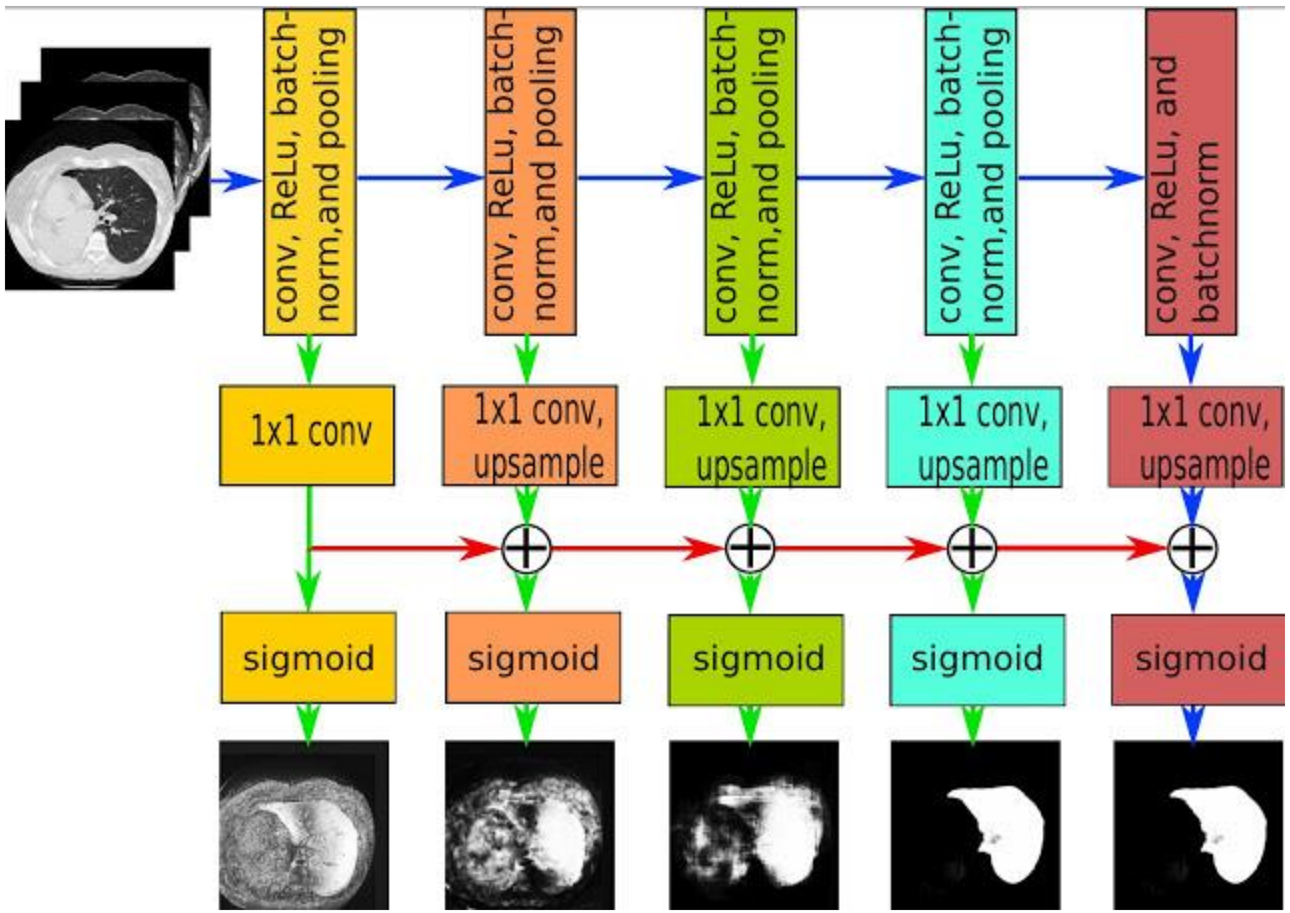

A. Harrison et al. *Progressive and Multi-Path Holistically Nested Neural Networks for Pathological Lung Segmentation from CT Images,* MICCAI 2017
https://adampharrison.gitlab.io/p-hnn/

Chest CT Lung Segmentation

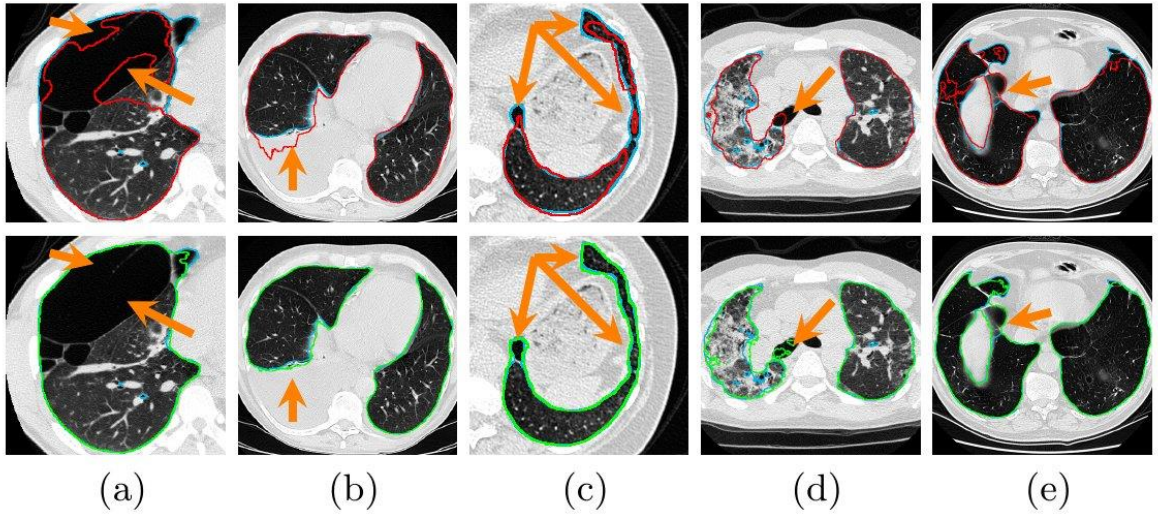

Fig. 2: Example masks of HNN and P-HNN, depicted in red and green, respectively. Ground truth masks are rendered in cyan. (a) HNN struggles to segment the pulmonary bullae, whereas P-HNN captures it. (b) Part of the pleural effusion is erroneously included by HNN, while left out by P-HNN. (c) P-HNN better captures finer details in the lung mask. (d) In this failure case, both HNN and P-HNN erroneously include the right main bronchus; however, P-HNN better captures infiltrate regions. (e) This erroneous ground-truth example, which was filtered out, fails to include a portion of the right lung. Both HNN and P-HNN capture the region, but P-HNN does a much better job of segmenting the rest of the lung.

A. Harrison et al. *Progressive and Multi-Path Holistically Nested Neural Networks for Pathological Lung Segmentation from CT Images,* MICCAI 2017

and more …

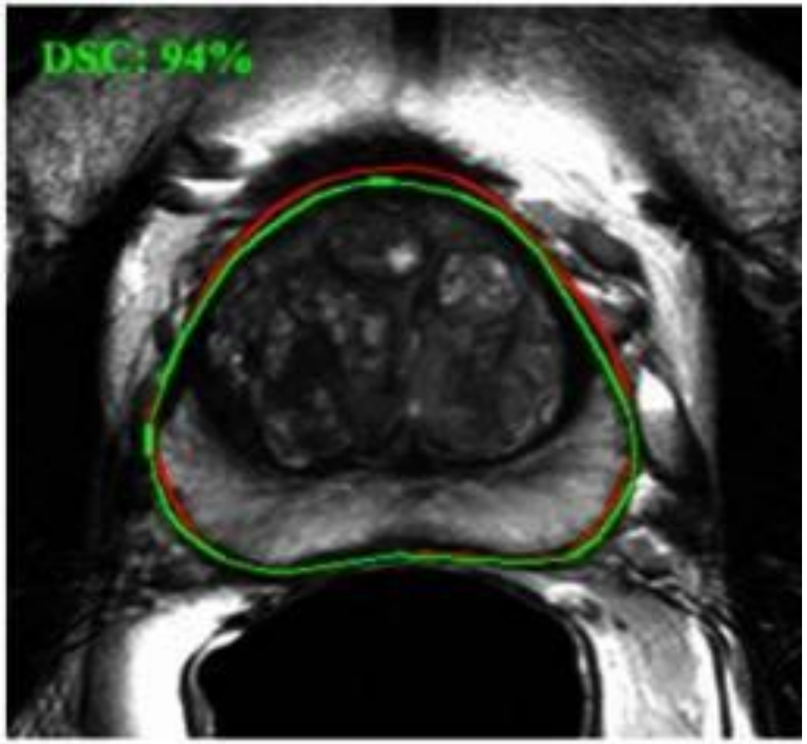

Prostate MRI

R. Cheng et al. JMI 2017

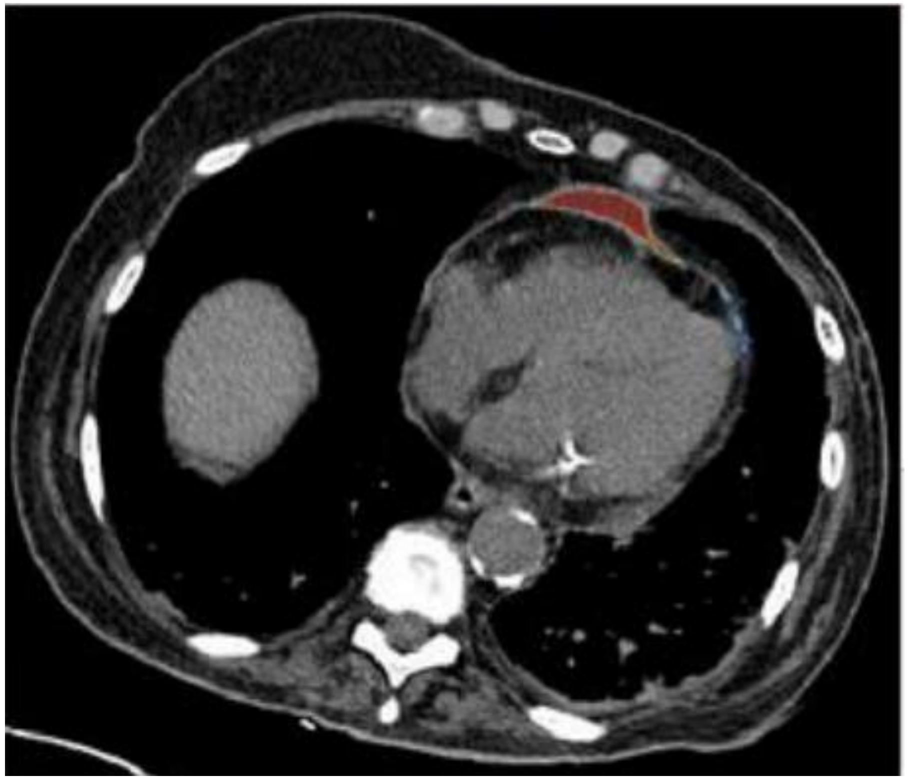

Pericardial effusion CT

J. Liu et al. ISBI 2017

Manual Annotation vs. Weak Supervision

- Pixel-wise annotation: laborious, time consuming
- Coarse annotation?
  - RECIST (Response evaluation criteria in solid tumors)

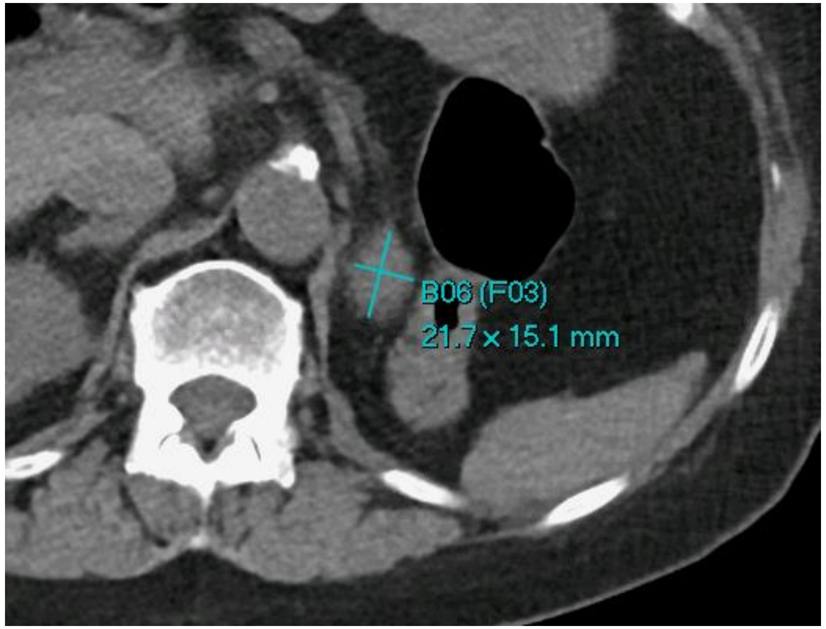

long-axis and short-axis

NIH National Institutes of Health
Turning Discovery Into Health

DeepLesion Dataset

- Mined from bookmarks (RECIST diameters) in NIH CC's PACS 32,120 axial CT slices from 10,594 studies of 4,427 unique patients
- 1–3 lesions in each image with size measurements (long-axis and short-axis)
- 32,735 lesions altogether

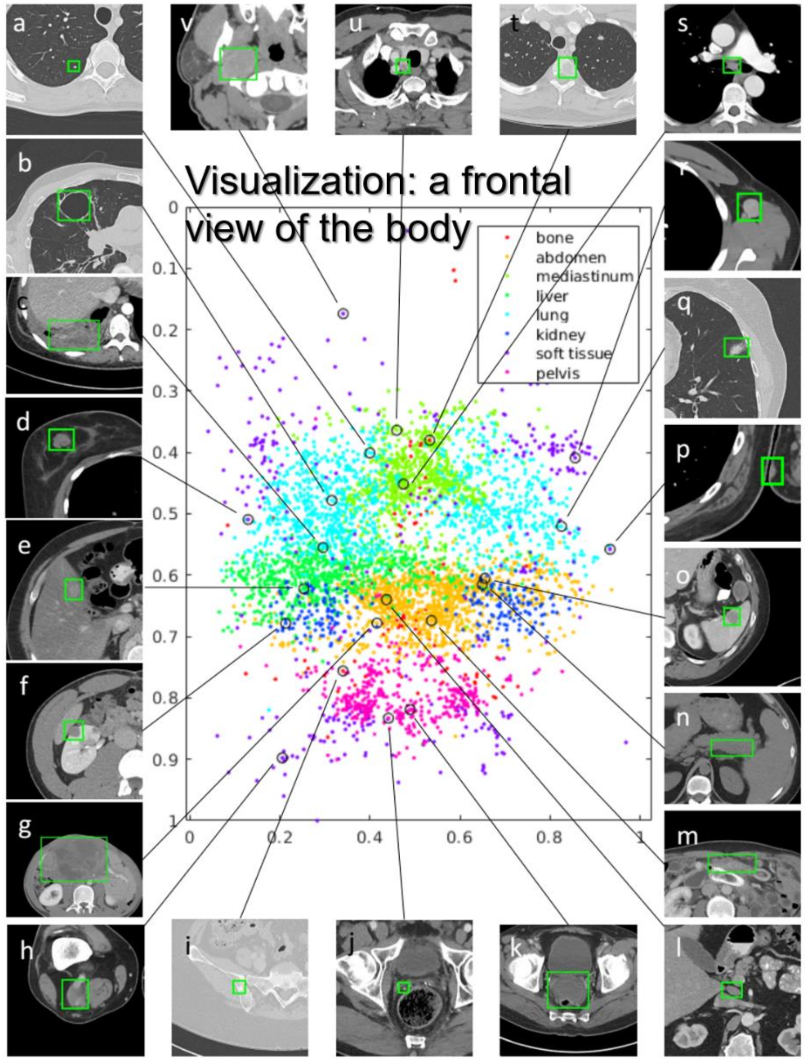

K. Yan et al. CVPR 2018, JMI 2018
https://nihcc.box.com/v/DeepLesion

Weakly Supervised Lesion Segmentation

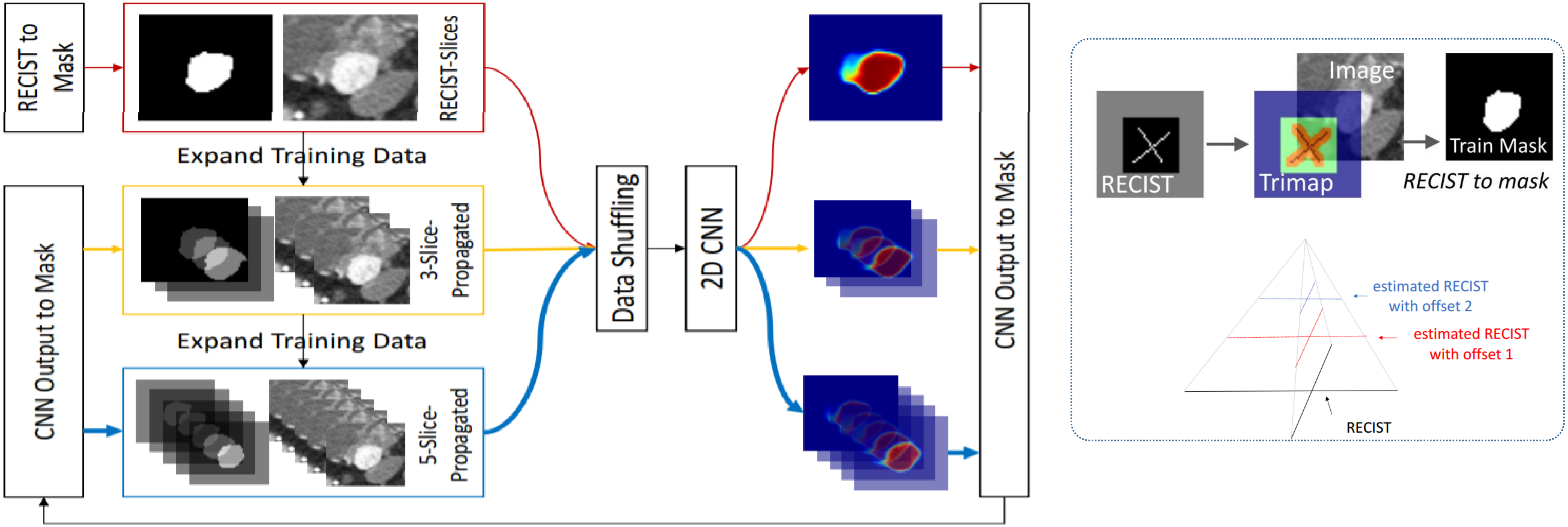

J. Cai, Y. B. Tang et al. *Accurate Weakly-Supervised Deep Lesion Segmentation using Large-Scale Clinical Annotations: Slice-Propagated 3D Mask Generation from 2D RECIST,* MICCAI 2018

Weakly Supervised Lesion Segmentation

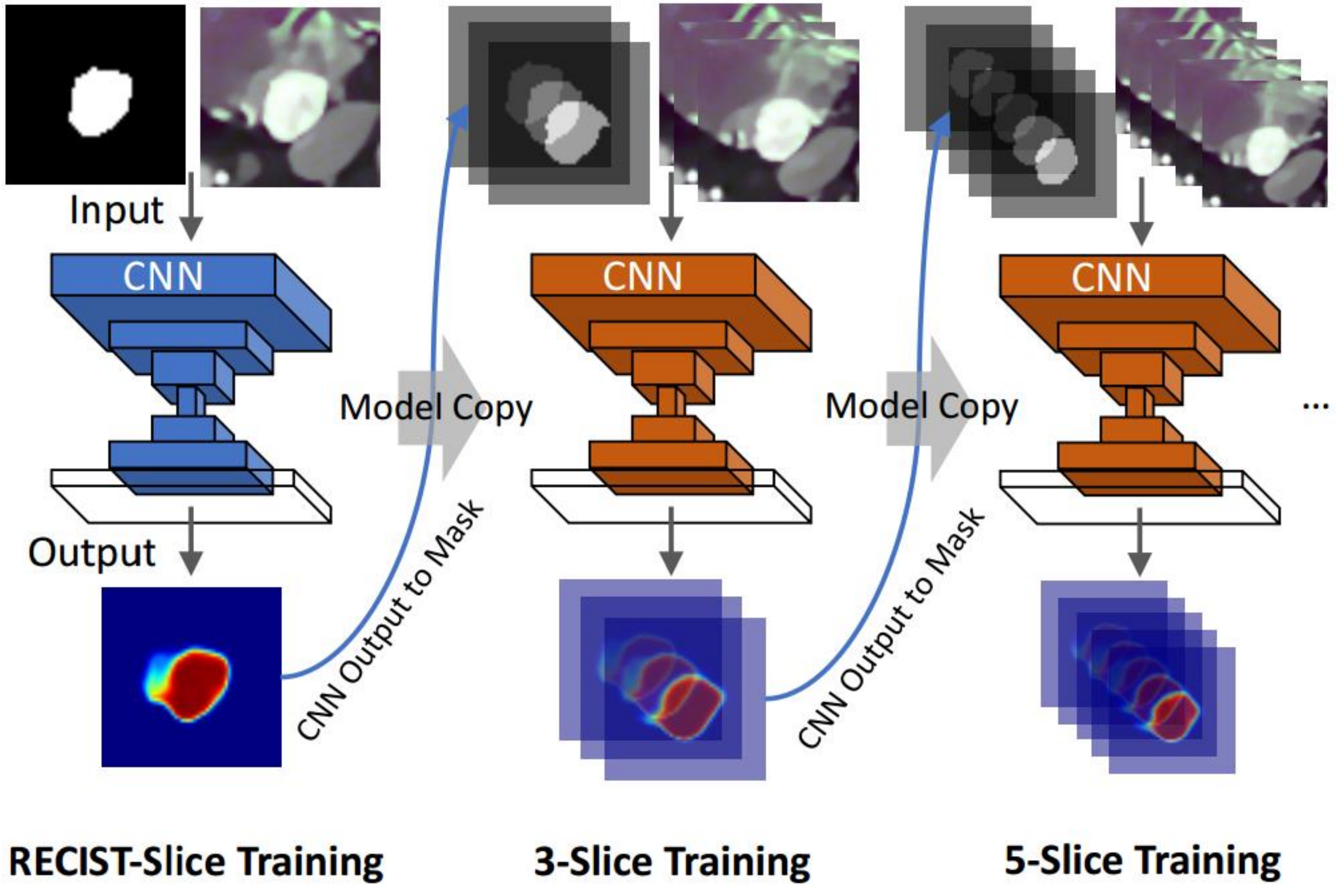

J. Cai, Y. B. Tang et al. *Accurate Weakly-Supervised Deep Lesion Segmentation using Large-Scale Clinical Annotations: Slice-Propagated 3D Mask Generation from 2D RECIST,* MICCAI 2018

Weakly Supervised Lesion Segmentation

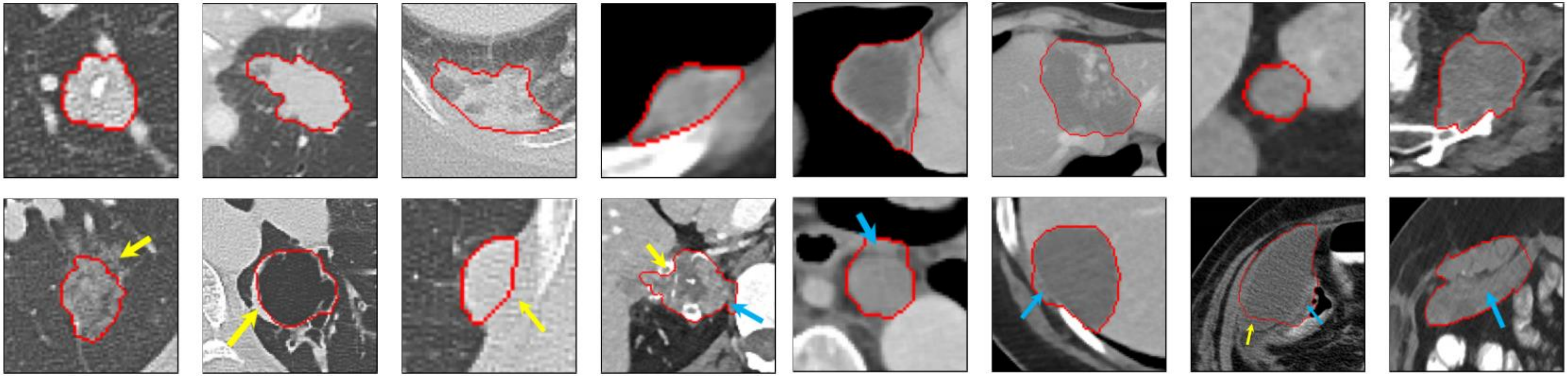

J. Cai, Y. B. Tang et al. *Accurate Weakly-Supervised Deep Lesion Segmentation using Large-Scale Clinical Annotations: Slice-Propagated 3D Mask Generation from 2D RECIST,* MICCAI 2018

Weakly Supervised Lesion Detection and Segmentation

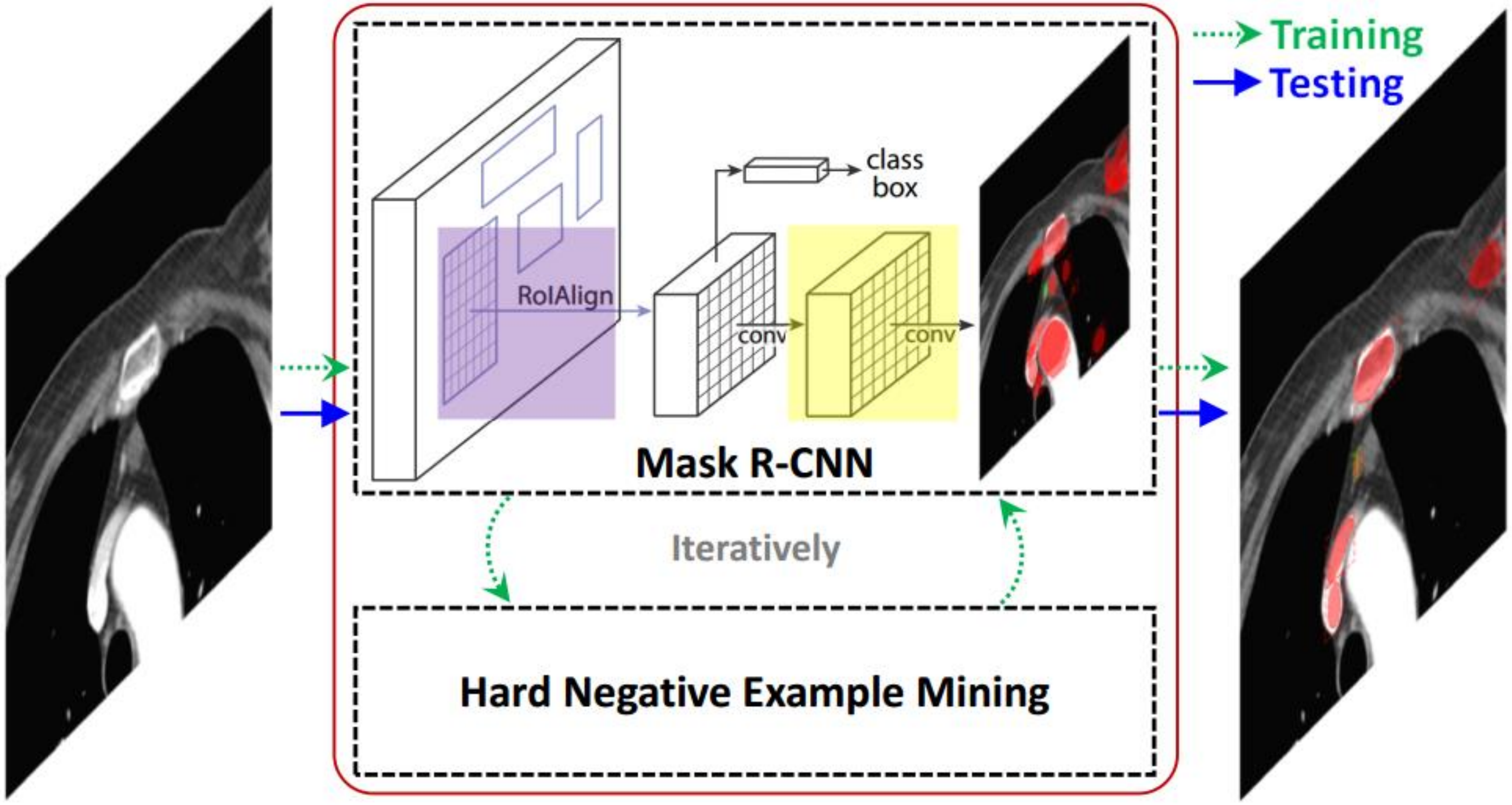

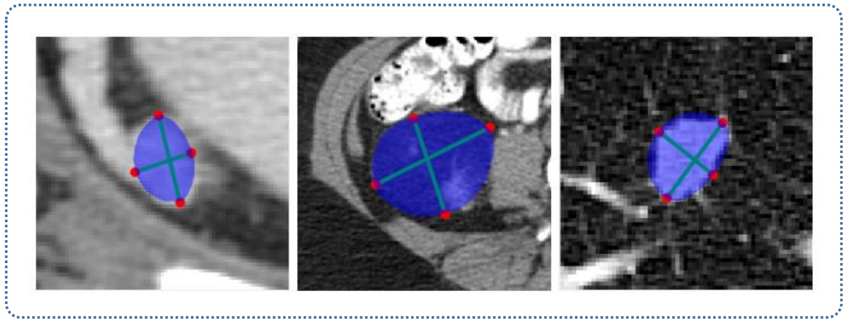

Y. Tang et al. *ULDor: A Universal Lesion Detector for CT Scans Enhanced Using Pseudo Masks and Hard Negative Example Mining,* ISBI 2019

Weakly Supervised Lesion Detection and Segmentation

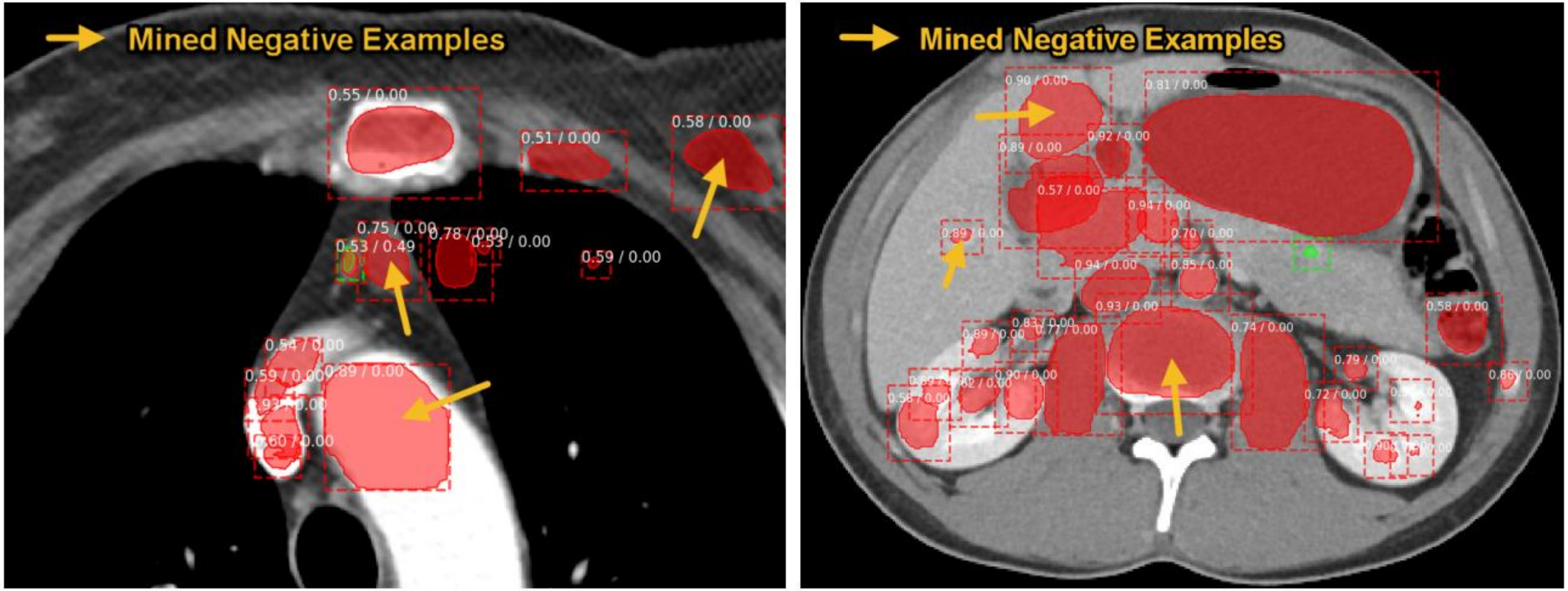

Y. B. Tang et al. *ULDor: A Universal Lesion Detector for CT Scans Enhanced Using Pseudo Masks and Hard Negative Example Mining,* ISBI 2019

Weakly Supervised Lesion Detection and Segmentation

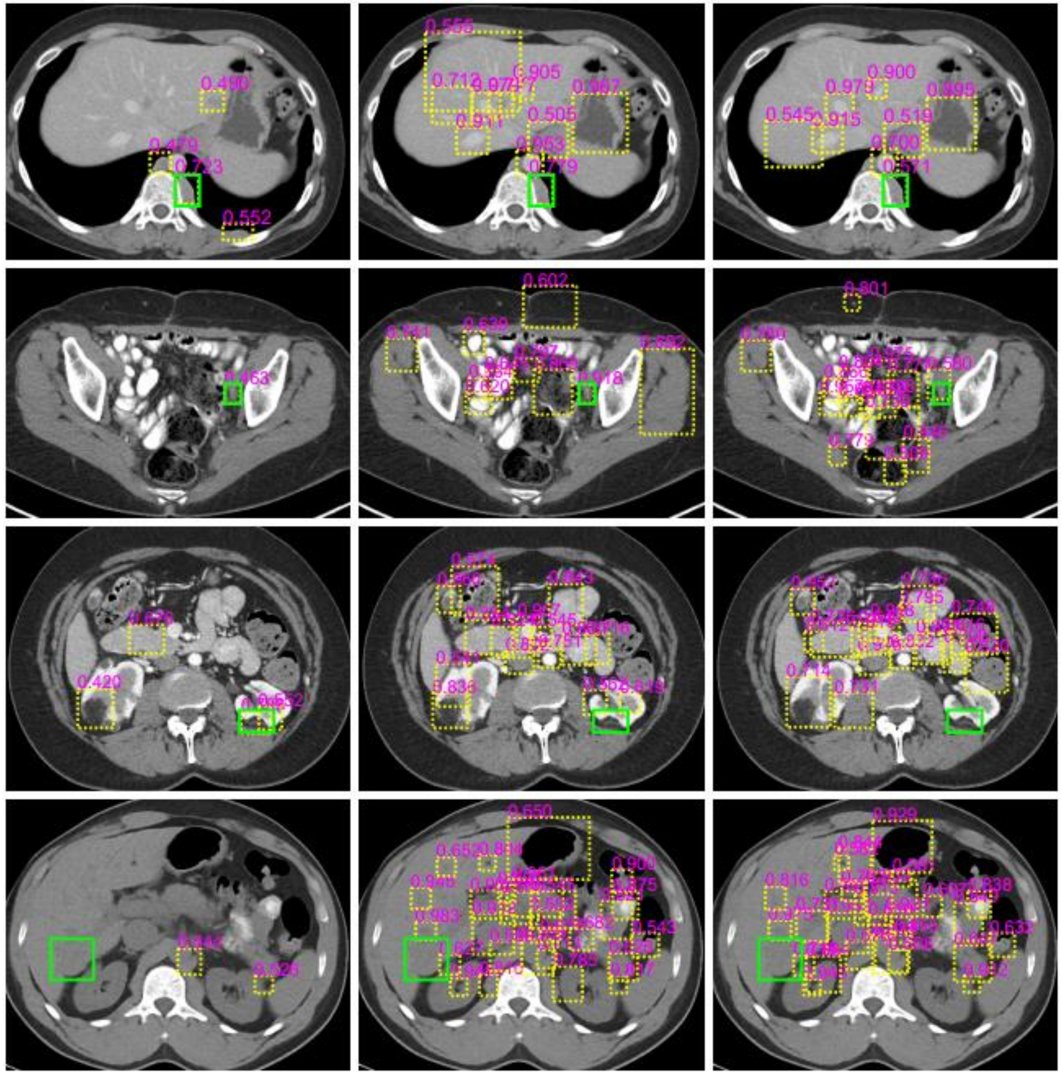

(a) (b) (c)

(a) Mask R-CNN + HNEM
(b) Mask R-CNN
(c) Mask R-CNN w/o Mask

Weakly Supervised Lesion Detection and Segmentation

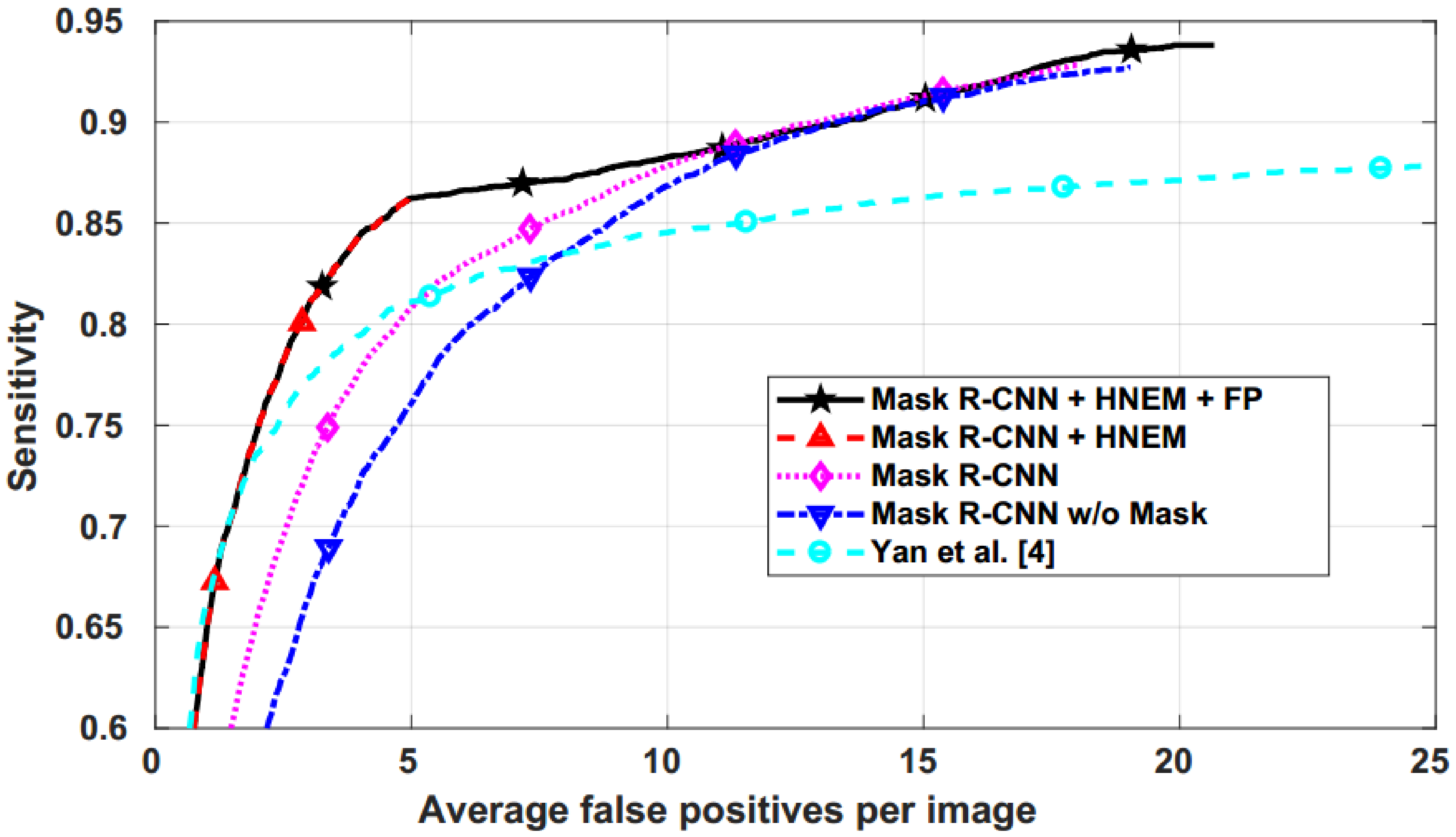

Y. B. Tang et al. *ULDor: A Universal Lesion Detector for CT Scans Enhanced Using Pseudo Masks and Hard Negative Example Mining,* ISBI 2019

Data Augmentation Using GANs

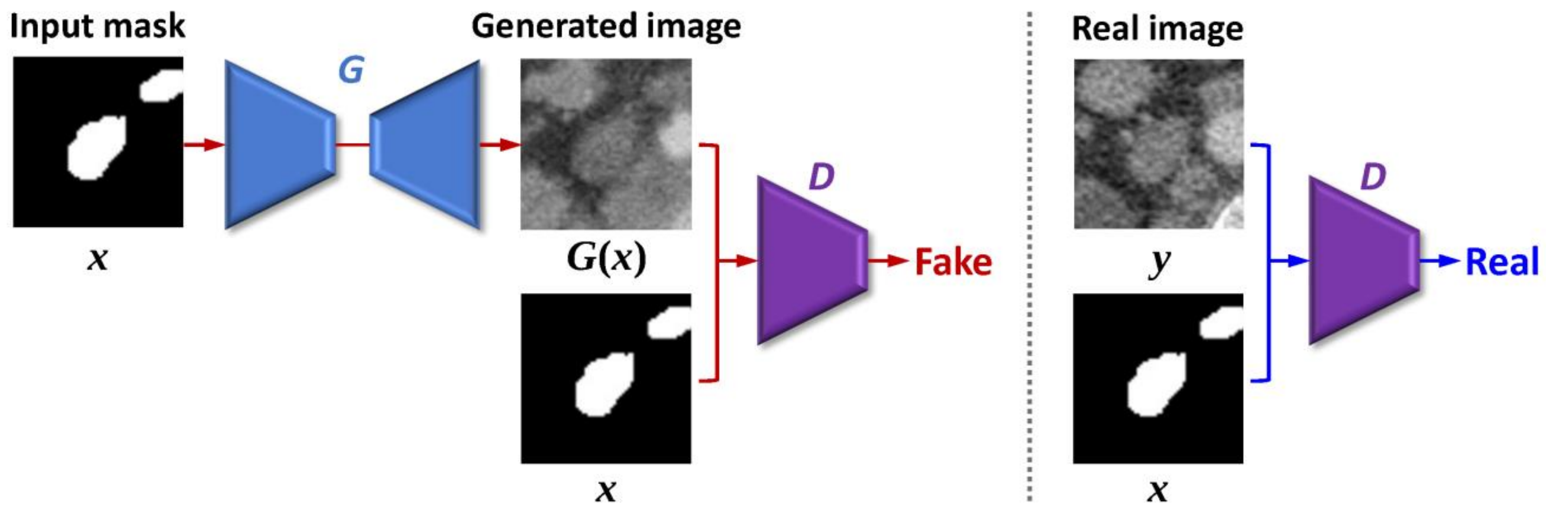

- CT-Realistic data augmentation (pix2pix GAN)
  - Training: real image & mask pairs as input
  - Inference:
    - Input: arbitrary lymph node masks (pseudo masks)
    - Output: synthesized (generated) CT images with “lymph nodes”

Y. Tang et al. *CT-Realistic Data Augmentation Using Generative Adversarial Network for Robust Lymph Node Segmentation*, SPIE Medical Imaging 2019

Data Augmentation Using GANs

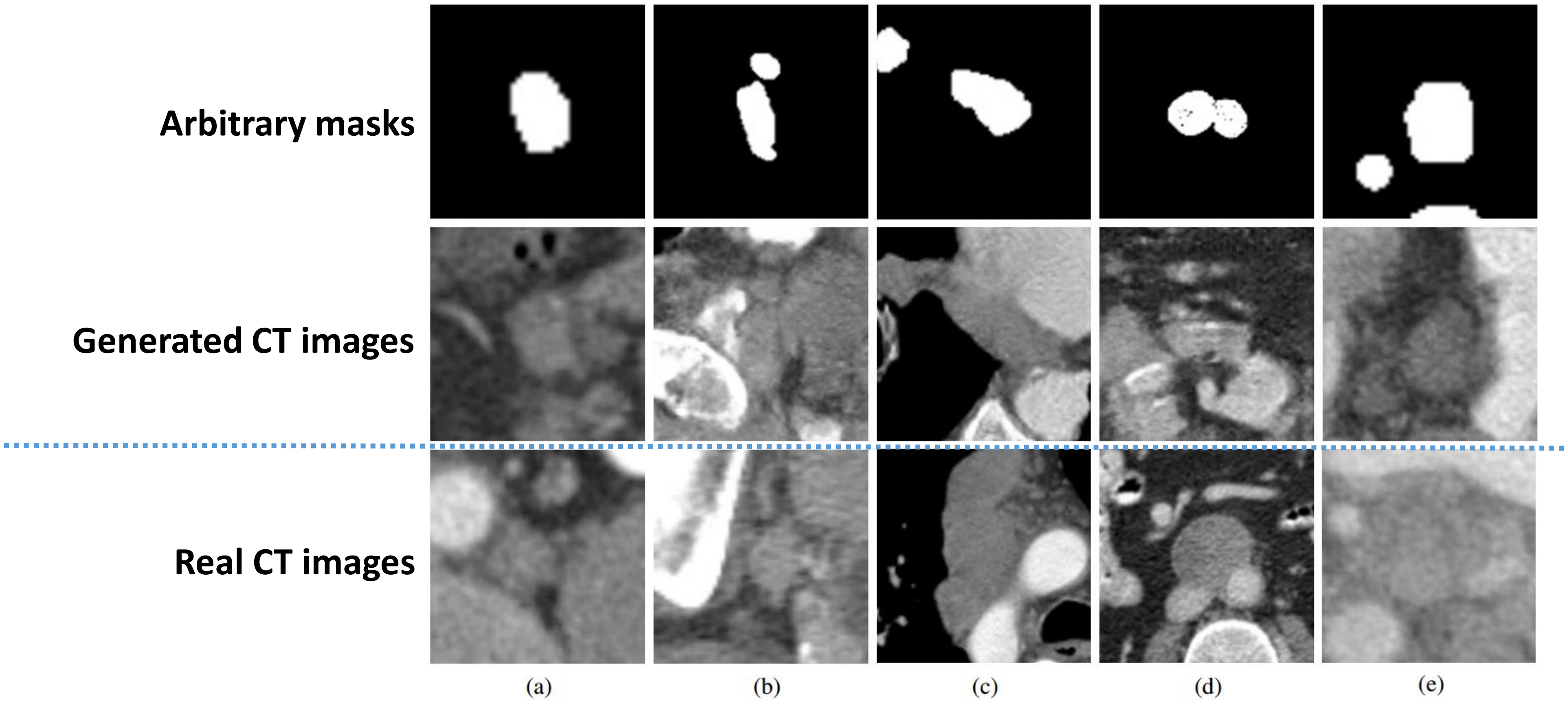

Y. Tang et al. *CT-Realistic Data Augmentation Using Generative Adversarial Network for Robust Lymph Node Segmentation*, SPIE Medical Imaging 2019

GANs Generated Images Improve Segmentation

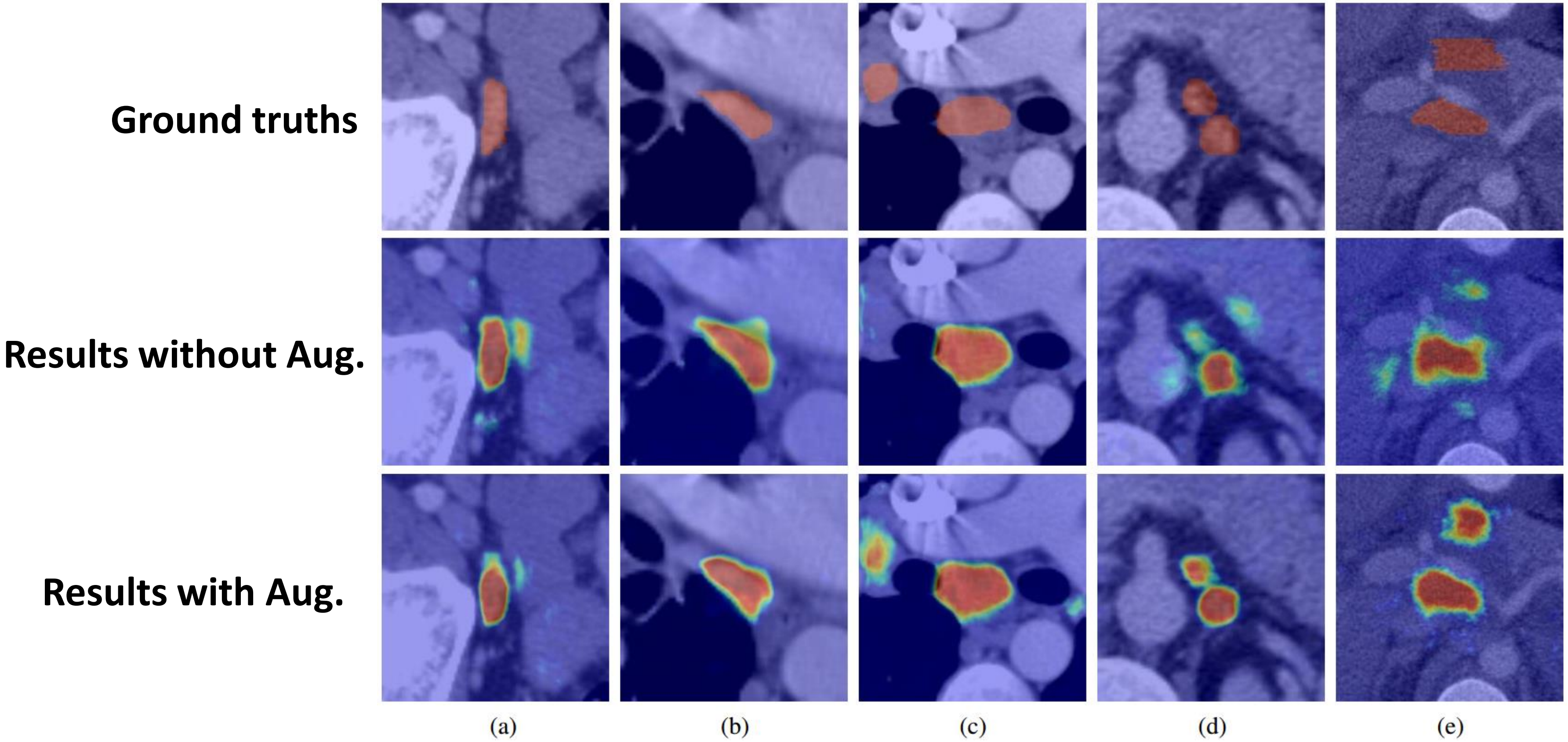

Strategy	Recall	Precision	Dice	AVD	VS
Without AAD	0.856 ± 0.128	0.783 ± 0.166	0.803 ± 0.130	2.306 ± 4.192	0.892 ± 0.113
With AAD_1	$\mathbf{0.857 \pm 0.120}$	0.803 ± 0.151	0.817 ± 0.118	1.957 ± 3.741	0.906 ± 0.096
With AAD_2	0.827 ± 0.125	$\mathbf{0.845 \pm 0.138}$	$\mathbf{0.825 \pm 0.112}$	$\mathbf{1.883 \pm 3.531}$	$\mathbf{0.912 \pm 0.091}$

Lung Segmentation on Chest Radiographs

Y. Tang et al. *XLSor: A Robust and Accurate Lung Segmentor on Chest X-Rays Using Criss-Cross Attention and Customized Radiorealistic Abnormalities Generation,* under open review

NIH ChestX-ray14 Dataset

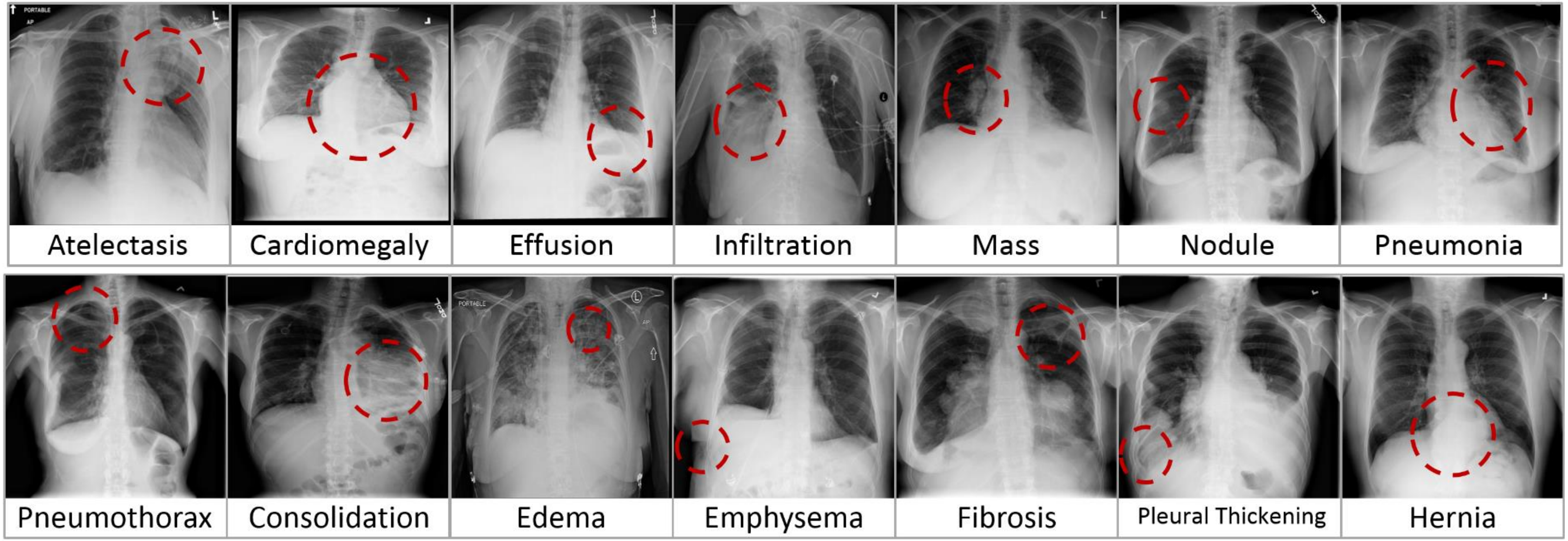

- 112,120 frontal-view chest X-ray images of 30,805 unique patients
- text-mined 14 disease image labels
- each image can have multiple labels

X. Wang et al. CVPR 2017
https://nihcc.app.box.com/v/ChestXray-NIHCC

Pathological Lungs are Harder to Segment

- To capture richer global contextual information for robust and accurate lung segmentation
- Especially for pathological lungs with less clear lung boundaries.

Y. Tang et al. *XLSor: A Robust and Accurate Lung Segmentor on Chest X-Rays Using Criss-Cross Attention and Customized Radiorealistic Abnormalities Generation,* under open review

Lung Segmentation with Data Augmentation

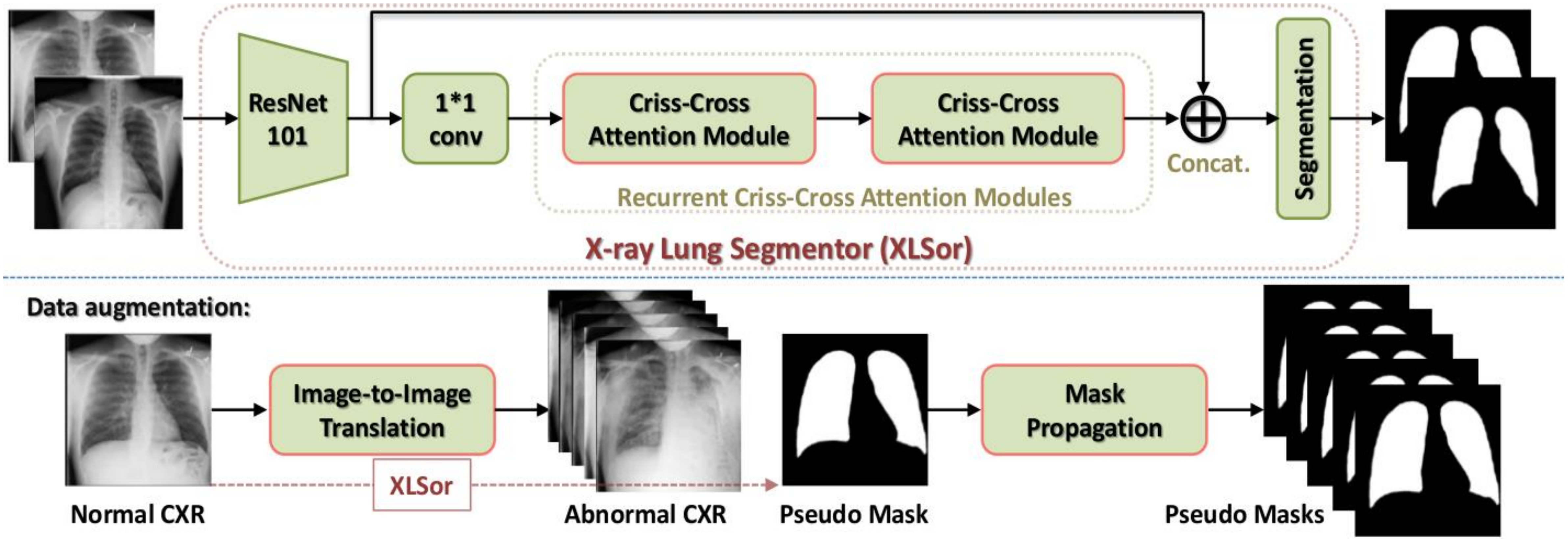

Y. Tang et al. *XLSor: A Robust and Accurate Lung Segmentor on Chest X-Rays Using Criss-Cross Attention and Customized Radiorealistic Abnormalities Generation,* under open review

Lung Segmentation with Data Augmentation

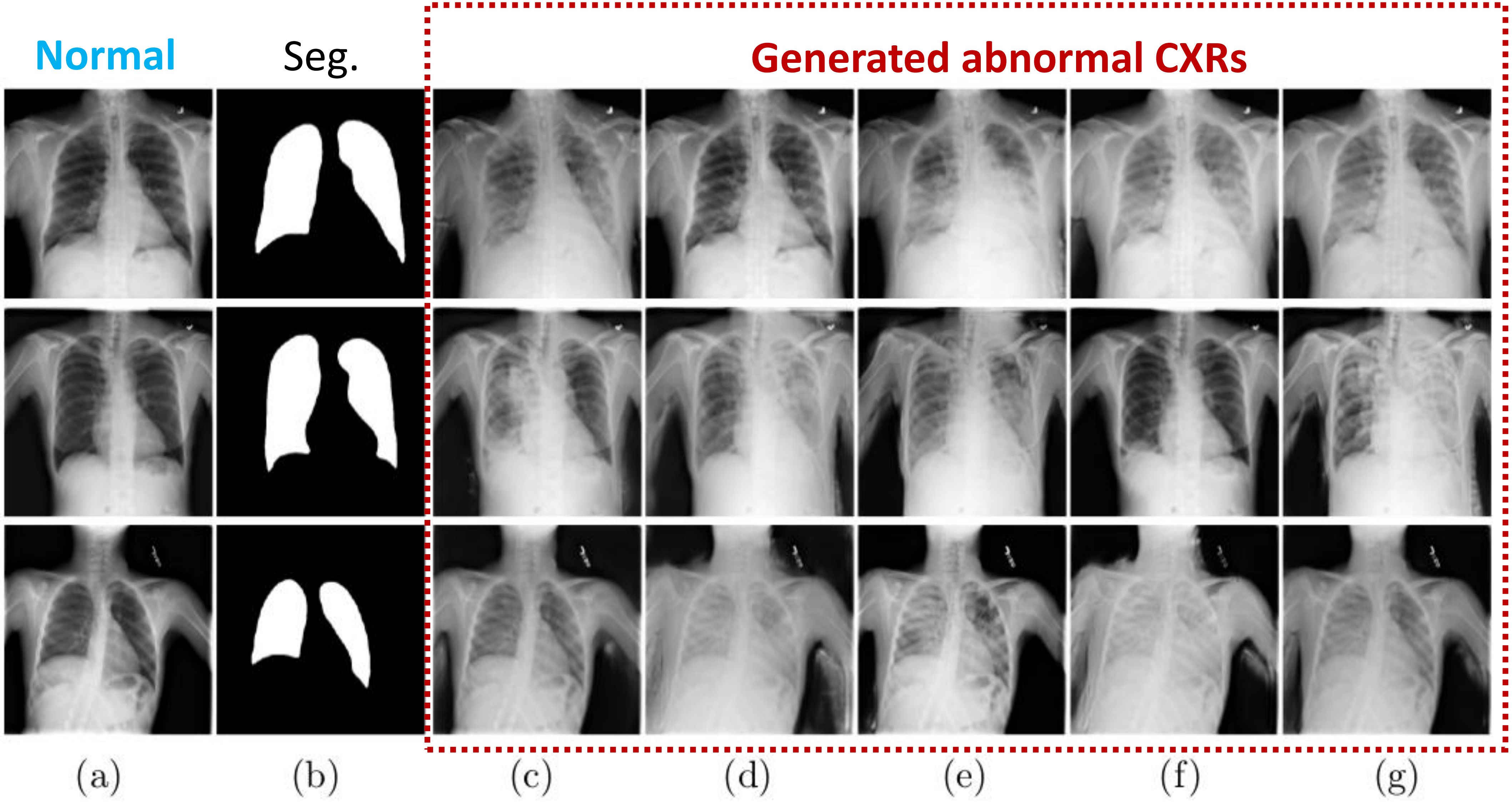

Segmentation Results on the NIH Dataset

Method	REC↑	PRE↑	DICE↑	AVD↓	VS↑
XLSor_{R}	0.966±0.02	0.927±0.09	0.943±0.05	0.669±1.64	0.966±0.05
XLSor_{R+A^1}	0.958±0.03	0.973±0.02	0.965±0.02	0.172±0.26	0.985±0.01
XLSor_{R+A^2}	0.962±0.02	**0.980±0.01**	0.971±0.01	0.097±0.08	0.989±0.01
XLSor_{R+A^3}	0.967±0.02	0.978±0.02	0.973±0.01	0.089±0.07	0.990±0.01
XLSor_{R+A^4}	**0.974±0.01**	0.976±0.01	**0.975±0.01**	**0.078±0.06**	**0.993±0.01**
XLSor_{A^4}	0.964±0.02	0.983±0.01	0.973±0.01	0.098±0.13	0.988±0.01
U-Net_{R}	0.938±0.07	0.761±0.20	0.823±0.16	5.231±9.02	0.869±0.15
U-Net_{R+A^1}	0.926±0.05	**0.960±0.03**	0.942±0.03	0.832±1.29	0.971±0.02
U-Net_{R+A^2}	0.947±0.04	0.950±0.04	0.948±0.03	0.500±1.03	0.981±0.02
U-Net_{R+A^3}	0.950±0.03	0.954±0.03	0.951±0.02	0.393±0.58	0.983±0.02
U-Net_{R+A^4}	0.943±0.04	0.958±0.03	0.950±0.03	0.454±0.73	0.982±0.02
U-Net_{A^4}	**0.952±0.03**	0.959±0.03	**0.955±0.02**	**0.315±0.47**	**0.983±0.02**

Y. Tang et al. *XLSor: A Robust and Accurate Lung Segmentor on Chest X-Rays Using Criss-Cross Attention and Customized Radiorealistic Abnormalities Generation,* under open review

Lung Segmentation with Data Augmentation

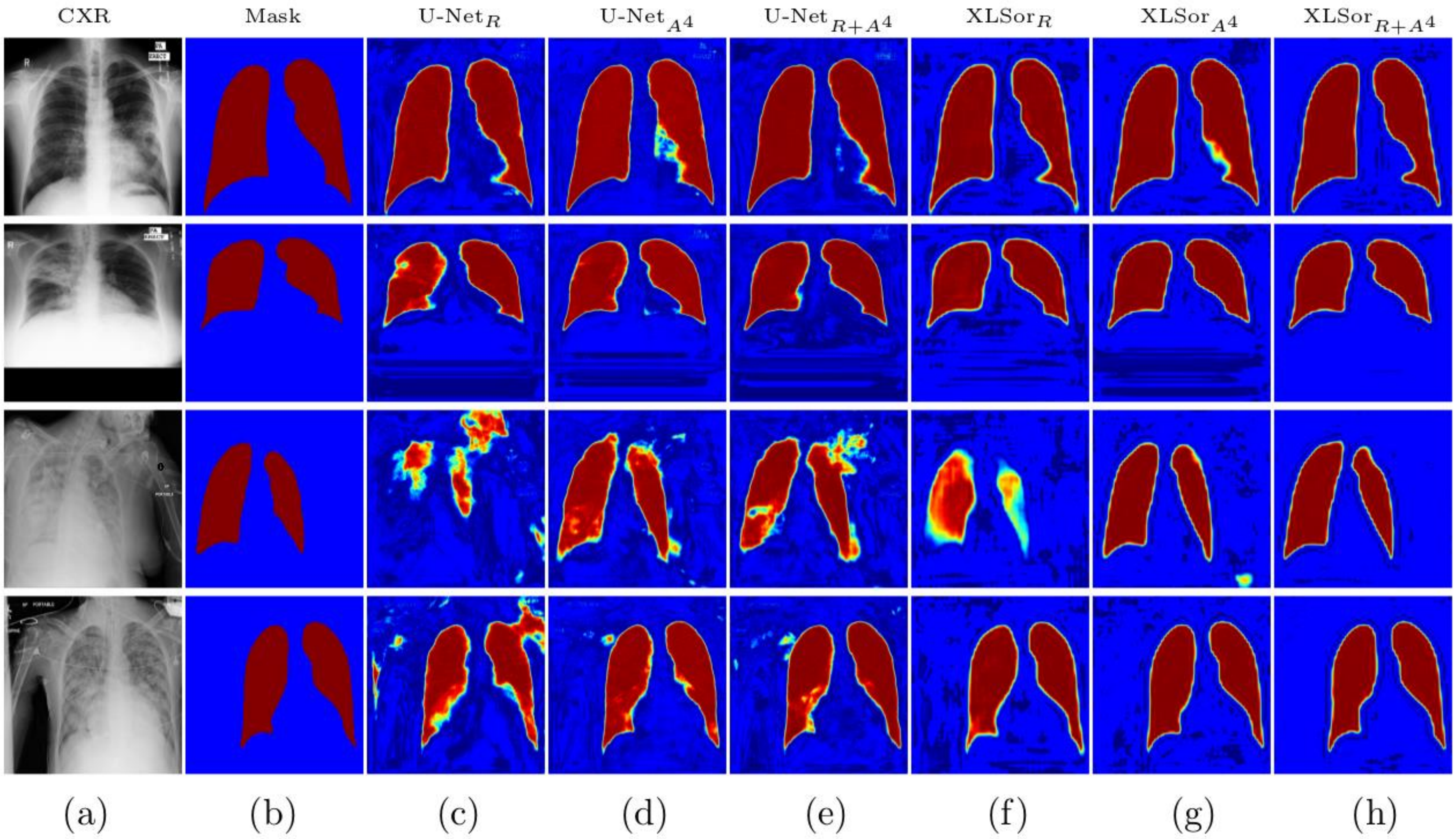

Take Home Messages

- Deep learning is powerful but data hungry
- Pixel-wise manual annotation on medical images is tedious
- Weak supervision is an alternative way (e.g., image level label, RECIST, etc.)
- Data augmentation using generative models can be helpful

Acknowledgement

- All current and previous members in the CAD lab and collaborators who contributed to the presented work

- NIH Fellowship Programs, NIH CRADA

- NVIDIA for GPU card donations

To learn more:

https://github.com/rsummers11/CADLab